

## Hydrogen Adsorption on Nickel (100) Single-Crystal Face. A Monte Carlo Study of the Equilibrium and Kinetics

Tomasz Panczyk,<sup>\*,†</sup> Paweł Szabelski,<sup>‡</sup> and Władysław Rudziński<sup>†,‡</sup>

*Institute of Catalysis and Surface Chemistry, Polish Academy of Sciences, ul. Niezapominajek 8, 30-239 Cracow, Poland, and Department of Theoretical Chemistry, Faculty of Chemistry, UMCS, pl. M. Curie-Skłodowskiej 3, 20-031 Lublin, Poland*

*Received: June 25, 2004; In Final Form: March 29, 2005*

We propose a model of the dissociative adsorption of hydrogen on nickel single-crystal face. In this model, we treat the Ni(100) surface as a strongly correlated energetically heterogeneous surface, because the density functional theory (DFT) studies indicate that hydrogen atoms may adsorb either on hollow sites (energetically more favorable, binding energy 48 kJ/mol H) or bridge sites with the binding energy less by 11 kJ/mol H. The essential assumption of the proposed model is that the dissociation of the hydrogen molecule is possible only over the topmost Ni atom, and the resulting H atoms may adsorb either on two free hollow sites (but the adjacent bridge sites must be free) or two bridge sites (the adjacent hollow sites must be free). If the above condition is not fulfilled, then the dissociation and adsorption are impossible. The second assumption is that the rate (probability) of the associative desorption is limited by the rate of diffusion of H atoms on the surface. This is because the two H atoms desorb, giving an H<sub>2</sub> molecule, only when they meet on two adjacent hollow–bridge sites. Our model recovers very well the behavior of the experimental equilibrium adsorption isotherms as well as kinetic isotherms. As a result, we stated that hydrogen atoms are not completely free on the surface, but they cannot also be considered localized at room and elevated temperatures. Additionally, while analyzing the kinetic adsorption isotherms, we stated that the rate-limiting step during the dissociative adsorption of H<sub>2</sub> is the disintegration of the activated complex and the subsequent adsorption of hydrogen atoms.

### Introduction

The adsorption of hydrogen on nickel single-crystal faces has been a matter of many experimental and theoretical studies. This is because nickel catalysts are commonly used in many industrial processes such as hydrogenation, hydrotreating, methanation, and steam reforming of hydrocarbons. Although most important features of this system have already been resolved, there are still some problems which require explanation.

There is general agreement that hydrogen adsorbs dissociatively on all low-index Ni surfaces and that such surfaces remain unreconstructed under H<sub>2</sub> exposure.<sup>1–6</sup> At room temperature (or above), H atoms adsorbed on Ni(100) do not show any ordering.<sup>1,3,4,6,7</sup> At temperatures below 250 K, some experiments have shown the existence of an ordered H layer.<sup>7</sup> The saturation coverage of the Ni(100) surface exposed to molecular H<sub>2</sub> is, at low temperatures (150–250 K), close to 1 ML with H atoms coordinated in the fourfold hollow sites.<sup>8–11</sup> There is, however, a lack of precise information about the saturation coverage at room temperature. It may be expected that this saturation value should be lower than 1 ML, because at temperatures above 250 K, the diffusion and desorption begin to play a significant role.<sup>7</sup> This conclusion is additionally supported by the discussion of results from different sources in the work by Christmann et al.<sup>4</sup> They suggest that the saturation coverage at room temperature should be in the range 0.25–0.94 ML. These saturation coverages correspond to the adsorption of H atoms on the surface, because the penetration of the subsurface region does

not occur when the H atoms come from the dissociation of molecular hydrogen to which the surface is exposed.<sup>12–14</sup>

Most of experiments concerning the H<sub>2</sub>/Ni(100) system were focused on flash desorption measurements.<sup>3,4,9,15</sup> They revealed a quite clear picture of the energetics of atomic H adsorption. The binding energy of hydrogen at low coverage (desorption temperature ca. 350 K) was estimated to be 96.6 kJ/mol H<sub>2</sub> (23 kcal/mol H<sub>2</sub>). This value agrees well with the recent results of the DFT (density functional theory) calculations<sup>1</sup> indicating that this state corresponds to adsorption on the fourfold hollow (HL) sites. However, the TPD (temperature-programmed desorption) results also show the presence of an additional low-energy peak which appears after adsorption at very low temperature and high exposure.<sup>3,4,9,15</sup> The binding energy of this state was estimated by Johnson and Madix<sup>15</sup> giving 69.7 kJ/mol H<sub>2</sub> (16.6 kcal/mol H<sub>2</sub>). The diffusion barrier for transition from the HL to the bridge (BR) site was estimated to be 110 meV,<sup>1</sup> so assuming that the adsorption energy on the HL site is 48.3 kJ/mol H, then the binding energy on the BR site should be around 37.7 kJ/mol H. The rather small difference between adsorption energies associated with the HL and BR sites (ca. 11 kJ/mol H) suggests that the adsorbed H atoms cannot be treated as localized; a small diffusion barrier allows for their movement on the surface even at quite low temperatures. On the other hand, the Ni(100) surface should be considered a strongly correlated energetically heterogeneous surface, because the H atoms may adsorb on the HL and BR sites as well. Thus, the thermodynamically available maximum coverage should be equal to 3 ML. However, such a high value of the coverage has never been observed experimentally. Moreover, an analysis of adsorption isotherms for this system

\* Corresponding author. E-mail: panczyk@vega.umcs.lublin.pl.

<sup>†</sup> Polish Academy of Sciences.

<sup>‡</sup> UMCS.

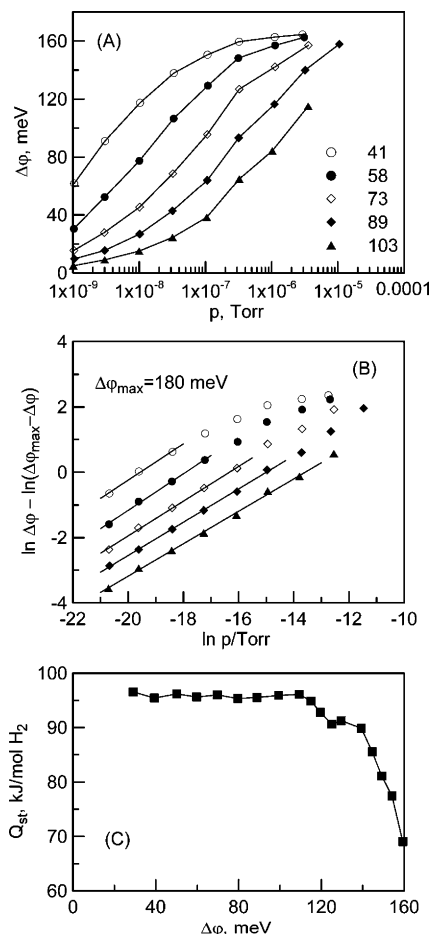


**Figure 1.** (A) The experimental adsorption isotherms of H<sub>2</sub> on Ni(100) at different temperatures shown in the legend in degrees Celsius. (B) The adsorption isotherms plotted as  $\ln \Delta\varphi/(\Delta\varphi_{\max} - \Delta\varphi)$  vs  $\ln p$  for different temperatures (symbols) and their linear regressions done for  $\Delta\varphi < 110$  meV (lines). (C) Isosteric heat of adsorption as a function of  $\Delta\varphi$  calculated using Clausius–Clapeyron equation.

indicates that their slopes change with the temperature. Only for higher temperatures do these slopes tend toward the theoretically correct limit for the dissociative adsorption (i.e., 0.5); for lower temperatures, they increase considerably, suggesting an order lower than two for the adsorption process.

Therefore, the aim of this work is to propose a model of adsorption of hydrogen on the Ni(100) surface which is able to explain the lower than unity saturation coverage at room temperature, the decreasing tendency of the slopes of adsorption isotherms with increasing temperature, and the existence of disordered surface structures at saturation for room and elevated temperatures.

**Experimentally Observed Features of the Hydrogen Adsorption Isotherms on Ni(100).** This apparently simple system appears to be rather complicated from the thermodynamic point of view. This expectation is confirmed by the analysis of adsorption isotherms and isosteric heats of adsorption reported by Christmann et al.<sup>4</sup> They also reported a set of flash desorption spectra (recorded in the range 25–200 °C) indicating only a single desorption peak with the desorption temperature decreasing with surface loading (such behavior is generally observed for second-order desorption process). The adsorption isotherms (Figure 1A) were recorded at temperatures between 41 and 182 °C, so they should account only for adsorption on one type of adsorption site (HL). Additionally, the shape of the isosteric heat of adsorption  $Q_{st}$  (Figure 1C) shows that adsorption

**TABLE 1: Values of the Slopes of Adsorption Isotherms Plotted in the Form  $\ln \Delta\varphi/(\Delta\varphi_{\max} - \Delta\varphi)$  vs  $\ln p$  for Different Values of  $\Delta\varphi_{\max}$**

temperature °C	$\Delta\varphi_{\max}$ 170 meV	$\Delta\varphi_{\max}$ 175 meV	$\Delta\varphi_{\max}$ 180 meV	$\Delta\varphi_{\max}$ 185 meV	$\Delta\varphi_{\max}$ 190 meV
41	0.593	0.573	0.556	0.540	0.526
58	0.581	0.570	0.559	0.550	0.541
73	0.544	0.537	0.531	0.525	0.520
89	0.519	0.514	0.509	0.505	0.501
103	0.511	0.505	0.500	0.495	0.491

energy is independent of the coverage up to  $\Delta\varphi < 110$  meV. This implies that for coverages  $\Delta\varphi < 110$  meV the adsorption isotherm should follow the Langmuir equation for dissociative adsorption.

The representation of the surface coverage via the work function change  $\Delta\varphi$  requires some comments. Christmann et al. showed<sup>4</sup> that  $\Delta\varphi$  is proportional to coverage at least up to  $\Delta\varphi < 85$  meV, while for higher values of  $\Delta\varphi$ , the proportionality no longer holds, and calibration of the slope of  $\Delta\varphi$  versus  $\theta$  may be smaller than that for  $\Delta\varphi < 85$  meV. However, looking at the shape of the  $Q_{st}$  function, we may expect that the full proportionality is kept even for  $\Delta\varphi = 110$  meV (i.e., the value where  $Q_{st}$  drops to lower values). Obviously, it is necessary to confine the analysis of the isotherms (represented as the work function changes) as well as the heats of adsorption (determined from these isotherms) to the values of  $\Delta\varphi$  not higher than 110 meV. For higher values of  $\Delta\varphi$ , the correlation between work function and coverage no longer exists.<sup>4</sup>

Thus, when plotting the experimental points of adsorption isotherms as  $\ln \Delta\varphi/(\Delta\varphi_{\max} - \Delta\varphi)$  versus  $\ln p$  (for  $\Delta\varphi < 110$  meV), one should obtain straight lines with slopes equal to  $1/2$ . Such plots always require some arbitrary choice of  $\Delta\varphi_{\max}$ . Figure 1B shows such plots for  $\Delta\varphi_{\max} = 180$  meV. It should be noted that  $\Delta\varphi_{\max}$  cannot be less than 170 meV (i.e., the maximum value of  $\Delta\varphi$  recorded at full saturation<sup>4</sup>).

As can be seen from Figure 1B, the linearity of the adsorption isotherms is excellent up to  $\Delta\varphi = 110$  meV; however, the slopes of these linear forms of the isotherms show rather strange behavior (Table 1). Although their strong dependence on  $\Delta\varphi_{\max}$  is rather obvious, their decreasing tendency with temperature cannot be explained on the basis of the Langmuir model of adsorption, which seemed to be appropriate in view of the behavior of the heat of adsorption.

It is also possible that the hydrogen atoms adsorbed on the Ni(100) surface should be considered fully mobile. Then, the Volmer adsorption isotherm<sup>16</sup> for dissociative adsorption should be applied. Our attempts to apply it, however, failed. The experimental points plotted in the form  $\ln \Delta\varphi/(\Delta\varphi_{\max} - \Delta\varphi) + \Delta\varphi/(\Delta\varphi_{\max} - \Delta\varphi)$  versus  $\ln p$  were not linear (except from the two lowest temperatures), and their slopes were even more temperature dependent. The values of the slopes never reached the theoretically correct value (i.e.,  $1/2$ ). This implies that the model of adsorption equilibria of hydrogen on Ni(100) is not as simple as expected and requires further thermodynamic analysis.

The experimental equilibrium adsorption isotherms as well as kinetic isotherms (recorded at constant temperature 300 K and five different pressures) were analyzed by Christmann et al.<sup>4</sup> They proposed a semiempirical kinetic equation which for infinite times gives an equilibrium adsorption isotherm. This equation has been developed under the assumption that the kinetics of adsorption is a first-order process, whereas the kinetics of desorption is second-order. Both equations were able to fit the experimental data points with moderate accuracy.<sup>4</sup>

However, Christmann's approach has been criticized by Halsey,<sup>17</sup> because it does not follow the requirement of detailed balance.

Another question is why the saturation coverage at room temperature is lower than 1 ML. From the DFT calculations,<sup>1,18</sup> it follows that the hydrogen atom can adsorb either on an HL site or a BR site and that the difference between binding energies on these sites is rather small (i.e., ca. 11 kJ/mol). This implies that the maximum coverage should be 3 ML (for sufficiently high chemical potential), but such high coverages have been never observed.

The experimental data concerning the kinetics of adsorption of H<sub>2</sub> on Ni(100) are rather rare. Rendulic et al.<sup>19</sup> have published a set of initial sticking coefficient curves obtained for different beam energies and angles of incidence. These data were satisfactorily explained by Kresse<sup>18</sup> who recovered them theoretically using DFT and molecular dynamics calculations. Christmann et al. published<sup>4</sup> kinetic curves (i.e., the adsorbed amount vs time of exposure) for five different pressures of hydrogen. In our recent publication,<sup>20</sup> these data were subjected to theoretical analysis based on application of the statistical rate theory (SRT).<sup>21,22</sup> Using this approach, we were able to predict the time dependence of the adsorbed amount without involving the precursor mediated adsorption mechanism. However, in view of the complex mechanism of adsorption in this system, we were not able to find an equation describing the coverage dependence of the chemical potential of adsorbed H atoms<sup>20</sup> (the chemical potential is a necessary input function in the SRT kinetic equation), and we had to apply some empirical equation for representation of the chemical potential. Today, the introduction of empirical equations is not satisfactory, because the availability of fast computers makes it possible to solve even very complex systems. Therefore, we designed a model of the dissociative adsorption of H<sub>2</sub> on Ni(100) and used the grand canonical Monte Carlo method to calculate the equilibrium adsorption isotherms. Next, we determined the coverage dependence of the chemical potential of the hydrogen atoms and used it to calculate the kinetic isotherms for this system.

**The Model.** The results of the DFT calculations, concerning the interaction of the H<sub>2</sub> molecule with the Ni(100) surface,<sup>18</sup> show that the most probable pathways for dissociation of the H<sub>2</sub> molecule are those with the center of mass of the H<sub>2</sub> over the top site. Other possible orientations of the H<sub>2</sub> molecule are less probable, because the molecule must cross significant activation barriers. When the molecule approaches the surface with the center of mass over the top site, it dissociates, and the resulting H atoms may adsorb either on the HL or BR sites. The potential energy curves for both situations are very similar, but the final energy gain is larger when the atoms end up in the more favorable hollow sites.<sup>18</sup> One can distinguish many ways to realize the mechanistic model of the H<sub>2</sub>/Ni(100) system. After a number of tested versions, we finally concluded that the following model is able to predict most of the experimentally observed features of the system under consideration.

Thus, we assumed that after dissociation the hydrogen atoms occupy two neighboring diagonally oriented HL sites or two neighboring BR sites oriented in line with the orientation of the dissociating molecule. Further, we assumed that the dissociation and adsorption of the H atom on the HL site is possible only if the neighboring BR sites are free, and similarly, adsorption on the BR site is possible only if the neighboring HL sites are free. Thus, the adsorbing molecule can dissociate only if it meets an ensemble of two free HL (BR) sites and in their nearest neighborhood there are no already adsorbed H

atoms on the BR (HL) sites. This physically means that the presence of the adsorbed H atom on either an HL or BR site modifies the local electronic structure of the substrate in such a way that the dissociation of the molecule over neighboring top sites is impossible. Unfortunately, we could not find suitable results of DFT calculations supporting this hypothesis; however, some indirect conclusions following from the available literature data may support it. After Kresse,<sup>18</sup> the nature of the interaction of the H<sub>2</sub> molecule with the Ni topmost atom is electrostatic at large distances from the surface. At closer distances, when the H—H bond breaking occurs, the major contribution is derived from the interaction of d<sub>xz</sub> and d<sub>yz</sub> electrons of the Ni atom with the H<sub>2</sub>  $\sigma$  orbital. The d<sub>xz</sub> and d<sub>yz</sub> orbitals are antisymmetric with respect to the H<sub>2</sub> molecule. They only experience the electrostatic potential of the H cores but no Pauli repulsion, because the occupied H<sub>2</sub>  $\sigma$  state is orthogonal to them. Thus, we suppose that, when there is already an adsorbed H atom in the neighborhood of the Ni atom, the state of the d<sub>xz</sub> and d<sub>yz</sub> orbitals changes. This will probably induce additional repulsive forces between the incoming H<sub>2</sub> molecule and the Ni atom. Also, the Pauli repulsion between H<sub>2</sub>  $\sigma$  and H 1s electrons may be responsible for these repulsive forces. Thus, we believe that the barrier for dissociation increases when the H atoms are present in the neighborhood of the Ni atom, and therefore, the assumption that the dissociation of the H<sub>2</sub> molecule is possible only when it interacts with a free topmost Ni atom is well-suited. Moreover, the results of our calculations show that the above assumption is necessary to achieve a good agreement between simulations and experiment.

After adsorption, the H atoms may either diffuse on the surface or desorb. The diffusion of the adsorbate species proceeds via jumps from the HL (BR) site into the BR (HL) site, but now, there are no restrictions concerning permitted local configurations. The moving atom can jump on a free site no matter whether the neighboring sites are occupied or not. The desorption can take place only when two H atoms meet on adjacent HL and BR sites. So, in our model, the rate of desorption is limited by the rate of diffusion.

Additionally, we assumed that there are no lateral interactions between adsorbed H atoms, as is suggested by the results of the DFT calculations.<sup>1</sup> For the (100) surface, the possible contribution of lateral interactions may only be electrostatic, but screening from the surface electrons reduces possible electrostatic repulsion so that the adsorption energy is essentially independent of coverage.

**Method of Calculations.** The calculations were based on application of the grand canonical Monte Carlo method (GCMC). The simulations were performed on a lattice of 100  $\times$  100 adsorption sites (corresponding to top, bridge, and hollow sites, Figure 2) with periodic boundary conditions. A small segment of the lattice is schematically shown in Figure 2. Because the adsorption on the top site is strongly energetically unfavorable, the simulations were performed only on the active sites (i.e., HL and BR).

A single Monte Carlo step involves the following sequence of events. At the beginning of the simulation, an active adsorption site is chosen at random. If the site is free, the dissociation/adsorption step is attempted, and if not, then the diffusion or desorption step is performed. When the dissociation and subsequent adsorption is attempted, the nearest neighborhood of the chosen free site is checked. If this site is of type HL, then the adjacent BR sites are checked, whereas if the free site is of type BR, then the adjacent HL sites are checked. If any of the checked sites is already occupied, then the dissocia-



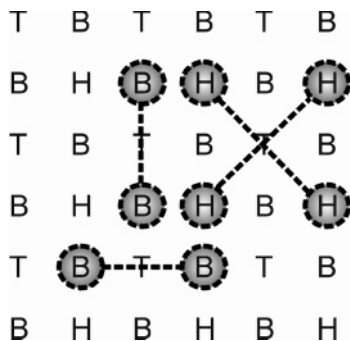


**Figure 2.** Schematic representation of the simulation lattice. T, top site (nickel atom); B, bridge site; H, hollow site. The dashed lines show possible configurations of the sets of HL–HL and BR–BR sites occupied after adsorption of the dissociated  $H_2$  molecule.

tion and adsorption is rejected. If all adjacent sites are free, then the second site needed for adsorption of the dissociated molecule is randomly chosen from the available set of configurations shown in Figure 2. If the second site also has no occupied adjacent sites, then the dissociation and adsorption of the two H atoms occur with the probability  $P_{\text{ads}}$

$$P_{\text{ads}} = \min\left(1, \exp\left(\frac{-2\epsilon_x + 2\mu_a}{kT}\right)\right) \quad (1)$$

where  $\epsilon_x$  is the energy of adsorption on site  $x$  (HL or BR), whereas  $\mu_a$  is the chemical potential of the adsorbed H atom. The DFT calculations showed that activation barriers are negligible when the  $H_2$  molecule approaches the surface with the center of its mass over the top site; therefore, we assumed that a molecule dissociates immediately when it strikes a suitable ensemble of sites.

When the randomly chosen active site is occupied, the diffusion of the H atom is attempted with the probability  $P_{\text{diff}}$ . To that purpose, a uniformly distributed random number  $r$  is generated, and when it is smaller than  $P_{\text{diff}}$  and the neighboring site is free, the adatom jumps with the probability  $\exp(-\Delta\epsilon/kT)$  onto a new adsorption site ( $\Delta\epsilon$  is the energy difference between new and old adsorption sites). When  $r > P_{\text{diff}}$ , the desorption of two adatoms is attempted. The desorption is possible only when two adjacent sites are occupied (i.e., HL–BR) and should occur with the probability  $P_{\text{des}}$

$$P_{\text{des}} = \min\left(1, \exp\left(\frac{\epsilon_H + \epsilon_B - 2\mu_a}{kT}\right)\right) \quad (2)$$

where  $\epsilon_H$  and  $\epsilon_B$  are the adsorption energies on the hollow and bridge sites, respectively. Equation 2, however, describes the probability of desorption of the two H atoms when no additional forces exist in the configuration HL–BR. Notice that in such a configuration the distance between the two H atoms is very short. This implies that these atoms should be considered rather as an  $H_2$  quasi-molecule. This molecule is oriented almost parallel to the surface normal, and as follows from the DFT studies,<sup>18</sup> this state is strongly energetically unfavorable. In turn, this leads to immediate desorption of this  $H_2$  molecule.

Therefore, we assumed that if the configuration HL–BR appears then the desorption of the  $H_2$  molecule occurs immediately (i.e., we forced  $P_{\text{des}} = 1$  in eq 2). Moreover, this assumption also restricts the increase of the coverage with the increasing chemical potential. Because, in this model, adsorption on the BR sites is allowed, the thermodynamical limit of the coverage (i.e., 3 ML) would always be reached for sufficiently high chemical potentials.

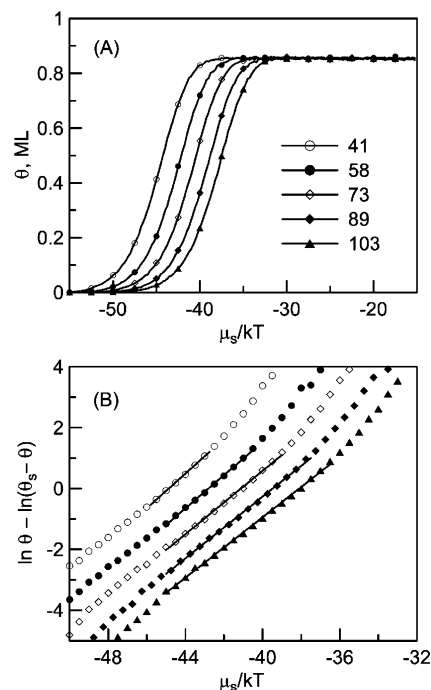


**Figure 3.** (A) The results of the MC simulation (solid lines) of adsorption isotherms at five temperatures (shown in the legend in degrees Celsius). (B) The adsorption isotherms from part A plotted in langmuirian form (symbols) and their linear regressions (lines) carried out for the same range of coverages as in Christmann's experiment.

The parameter  $P_{\text{diff}}$  (the probability of choosing the diffusion step) describes the relative rate of diffusion. It may be defined as the ratio of the diffusion rate to the desorption rate. The value of the parameter  $P_{\text{diff}}$  changes the slopes of the adsorption isotherms.

For a given value of the chemical potential,  $3 \times 10^8$  Monte Carlo steps were performed starting from the configuration obtained for the preceding value of  $\mu_s = 2\mu_a$ . In this way, we determined the average surface coverage as a function of the chemical potential of the adsorbed H atoms. The final adsorption isotherm was obtained by averaging the results of ten independent runs. The isosteric heat of adsorption was determined from differentiation of the total energy,  $E_{\text{tot}}$ , of the adsorbed phase

$$Q_{\text{st}} = \frac{d\langle E_{\text{tot}} \rangle}{d\langle N \rangle} \quad (3)$$

where  $\langle N \rangle$  is the average number of adsorbed H atoms.

The accepted value of the adsorption energy on the HL sites  $\epsilon_H = -48$  kJ/mol H is in agreement with the experimental results concerning the high-energy state of the H atoms, whereas  $\epsilon_B = -37$  kJ/mol corresponds with the results of the DFT calculations concerning the diffusion barrier between the HL and BR sites. The parameter  $P_{\text{diff}}$  was treated as an adjustable parameter (it is only one unknown parameter in the model), and its value was estimated after a number of trials, finally giving a good agreement between the simulations and the experimentally observed features of the system  $H_2/\text{Ni}(100)$ .  $P_{\text{diff}}$  was estimated to be  $0.04 \pm 0.02$ .

## Results and Discussion

**Adsorption Equilibrium.** Figure 3A shows the results of the MC simulation of the adsorption isotherms at five temperatures corresponding to Christmann's experiment.<sup>4</sup> First, let us concentrate on the qualitative behavior of the calculated

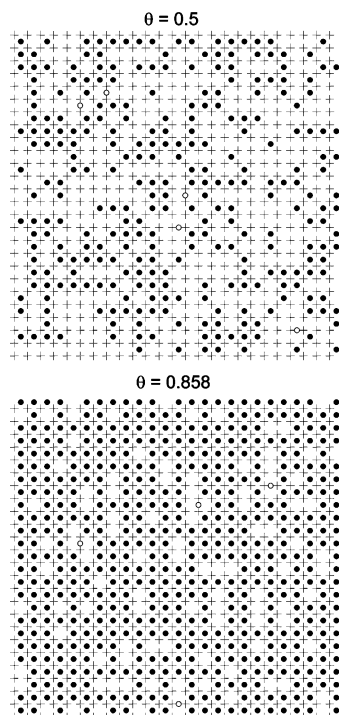


**Figure 4.** The snapshots of the surface structures at  $\theta = 0.5$  and at saturation  $\theta = 0.858$  taken at  $T = 73$  °C. The plus signs (+) indicate the positions of Ni atoms; the filled circles show the positions of H atoms adsorbed on hollow sites, whereas the open circles show the positions of H atoms adsorbed on bridge sites.

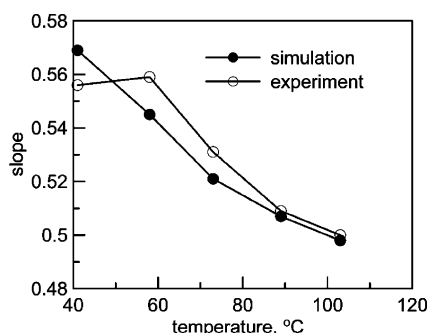


**Figure 5.** The comparison between the slopes of linear segments of adsorption isotherms shown in Figure 3B and the slopes determined from experimental adsorption isotherms (Figure 1B) assuming that  $\Delta\varphi_{\max} = 180$  meV.

isotherms. At the investigated temperatures, the saturation coverage is constant and equal to 0.858 ML. This value is in agreement with experimental findings as discussed in the Introduction section.

The snapshots of the surface structures at  $\theta = 0.5$  and at saturation  $\theta = 0.858$  shown in Figure 4 suggest that the adsorbed layer is not ordered and that the hydrogen atoms are present on the BR sites for all coverages. Their ratio, however, is very small, giving a negligible contribution to the heat of adsorption. Figure 4 represents the static pictures of surface structures, so one has to remember that the local ordering which can be seen in Figure 5 is only apparent.

Our observations of the surface structures during simulations showed that the hydrogen atoms adsorbed on the BR sites act only as an intermediate state for diffusion and desorption. When the occupation of the BR sites occurs (as a result of dissociation), the H atoms are immediately directed into neighboring free HL sites. Similarly, when an H atom jumps onto a BR site as a

result of diffusion, it may either jump into the neighboring free HL site (without any energetic barrier) or immediately recombine with the second H atom, adsorbed on the neighboring HL site, giving an  $H_2$  molecule. Although the lifetimes of the H atoms adsorbed on the BR sites are very short, it is necessary to account for their presence in the model. This is because the temperature dependence of the adsorption isotherms can be explained in this way. At lower temperatures, the probability of jumping of the H atoms decreases strongly. As a result, the adsorbed phase becomes localized and forms an ordered structure ( $1 \times 1$ ). Moreover, the adsorption becomes irreversible at low temperatures.

In Figure 3B, we show the isotherms from Figure 3A plotted in coordinates  $\ln \theta / (\theta_s - \theta)$  versus  $\ln p$  (i.e., showing the potential applicability of the Langmuir model of adsorption as suggested by Figure 1B). Of course, the isotherms are not linear in the whole range of coverages. Remembering that the experimental adsorption isotherms were determined in a rather narrow range of coverages and applying the same ranges to our simulated isotherms, we can find fairly linear segments on the isotherms (solid lines). To determine the absolute values of experimental coverages, we assumed  $\Delta\varphi_{\max} = 180$  meV. As can be seen, the slopes of these linear segments decrease with the temperature. This decreasing tendency can be explained in the following way: As the temperature increases, the concentration of the intermediate states for desorption also increases, because the probability of jumps from the HL sites into BR sites increases. Thus, the rate of desorption becomes higher and the isotherm less steep.

Figure 5 shows the comparison between experimentally determined slopes of the isotherms and the slopes estimated from simulations. Generally, the agreement is rather good, although some quantitative discrepancies are visible. This is not surprising, because the choice of  $\Delta\varphi_{\max}$  and the range of coverages used for the estimation of the slopes from the theoretical isotherms are rather arbitrary. However, the decreasing tendency of the slopes with increasing temperature is well-resolved. The only exception is the first point at  $T = 41$  °C, but one should remember that at this temperature only three experimental data points are available; this, in turn, makes the value of the determined slope uncertain.

The most important influence on the values of the slopes has the relative rate of diffusion  $P_{\text{diff}}$ . For  $P_{\text{diff}}$  of the order 0.1 and higher, the slopes of all the isotherms are practically equal to 0.5 with negligible temperature dependence. However, for  $P_{\text{diff}} < \sim 0.02$ , the slopes for the lowest temperatures are too high (of the order 0.8), and they decrease with temperature rather strongly, but for higher temperatures, they do not reach the value 0.5 as observed in the case of experimental isotherms. The estimated value of  $P_{\text{diff}} = 0.04$  implies that the diffusion of H atoms on the surface is not completely free; although the energetic barriers for diffusion are small, there are also other factors which hinder the motion of adatoms. This conclusion is supported by the analysis of the frequency factors, determined from the flash desorption spectroscopy by Christmann et al.<sup>4</sup>

Thus, from the above considerations, it follows that our model describes well all of the general features of the system  $H_2/Ni(100)$ . Moreover, the quantitative predictions are also in agreement with the experiment. Let us look in Figure 6A where the experimental and theoretical adsorption isotherms are plotted. The solid lines are the isotherms from Figure 3A expressed now as functions of pressure. Because we consider adsorption at very low pressure, we assumed a simple relation between the chemical potential  $\mu_s$  of the adsorbed species

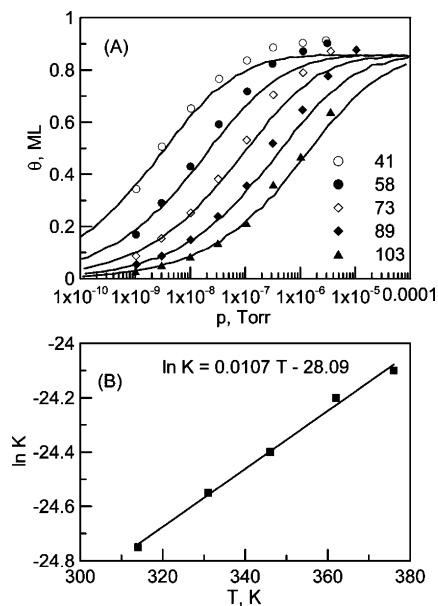


**Figure 6.** (A) The comparison between experimental (symbols) and theoretical adsorption isotherms for the adsorption temperatures shown in the legend in degrees Celsius. The  $\Delta\varphi_{\max}$  value, which is needed for calculation of the experimental coverage, was assumed to be 180 meV. (B) The temperature dependence of  $\ln K$  determined from fitting the theoretical adsorption isotherms to the experimental values.

and the pressure of gaseous phase  $p$

$$\ln p = \mu_s/kT - \ln K \quad (4)$$

where  $K$  may be defined as the function of the standard chemical potential  $\mu_s^\circ$  of the gas phase and the partition function of the adspecies concerning their internal degrees of freedom,  $q_{\text{int}}$ , that is

$$K = q_{\text{int}}^2 \exp\left(\frac{\mu_g^\circ}{kT}\right) \quad (5)$$

Thus, adding to  $\mu_s/kT$  a certain number ( $-\ln K$ ) at a constant temperature, we directly obtain  $\ln p$ . The particular value of  $-\ln K$  can be determined by comparing the theoretical and experimental adsorption isotherms. In this way, we obtained the values of  $\ln K$  for all the temperatures, assuming, as before,  $\Delta\varphi_{\max} = 180$  meV.

As can be seen in Figure 6B,  $\ln K$  is almost temperature independent, and its variation with temperature can be extrapolated using a straight line.

The agreement between theoretical and experimental adsorption isotherms is excellent up to  $\theta = 0.5$ – $0.6$  ML. For higher coverages, some discrepancies appear, especially for the two lowest adsorption temperatures. Let us recall that the experimental values of the coverage are represented in terms of the work function changes. As mentioned, Christmann et al. strongly underlined that the work function changes are directly proportional to the coverage only up to  $\Delta\varphi_{\max} = 100$  meV, which corresponds to approximately  $1/2$  ML. So, the disagreement for  $\theta > 1/2$  is obvious, because the experimental data cannot be correctly converted into the coverage in this range of work function values.

Similar disagreement between simulations and experiment for high coverages can also be observed in the heat of adsorption (Figure 7). Previously,<sup>20</sup> we attributed the decrease of the  $Q_{\text{st}}$  function for  $\Delta\varphi$  around 110 meV mainly to the onset of adsorption on less-energetic BR sites. The present results do

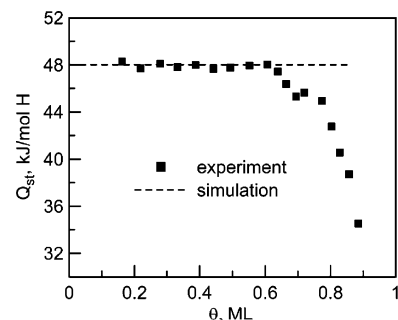


**Figure 7.** Heat of adsorption of hydrogen on Ni(100). Comparison between simulation and experiment. The experimental coverage was calculated assuming  $\Delta\varphi_{\max} = 180$  meV.

not support this thesis, because the occupation of the bridge sites is very small at all coverages. So, the heat of adsorption should be constant. However, the experimentally determined heat of adsorption<sup>4</sup> reveals a decreasing tendency before the saturation.

It is very difficult to understand why the experimentally determined heat of adsorption (from the Clausius–Clapeyron equation) decreases with coverage before the saturation. One may speculate that this effect is due to some energetic heterogeneity of the surface induced by impurities. It is, however, in contradiction with the behavior of the adsorption isotherms, because for energetically heterogeneous surfaces, the slopes of adsorption isotherms increase with temperature.<sup>23</sup> It is also possible that the decrease of the heat of adsorption close to saturation is due to repulsive interactions between the adsorbed species or to the decrease of the binding energy between the hydrogen atom and the adsorption site with increasing coverage. Both of these factors were not included in our model, because we relied mainly on the results of the DFT studies while building up this model. As mentioned, the DFT calculations do not suggest the existence of these repulsive interactions, and the change of the binding energy of the hydrogen atoms with increasing coverage is negligibly small.

Thus, we believe that the most probable source of the behavior of the experimental heat of adsorption is the lack of proportionality between  $\Delta\varphi$  and  $\theta$  for the coverages close to the saturation.

**Adsorption Kinetics.** The problem of the kinetics of dissociative adsorption has already been thoroughly investigated by us.<sup>20,24</sup> Particularly, the kinetics of hydrogen dissociative adsorption on the Ni(100) surface has been a matter of our recent publication.<sup>20</sup> Application of the SRT approach for prediction of the adsorption kinetics requires determination of the chemical potentials of the gas and adsorbed phases. As mentioned, in ref 20, we used an empirical equation describing the chemical potential of the adsorbed H atoms, because the complex features of this system made it impossible to find a simple theoretical expression which would be able to account for them.

Therefore, it is necessary to revise the previously obtained results concerning the kinetics of adsorption. However, our present investigations show that most of the previous conclusions are still valid, and the small differences only come from the application of different techniques of calculations.

The SRT approach postulates that the time evolution of the coverage can be described by the following master equation

$$\frac{d\theta}{dt} = K'_{\text{gs}} \left[ \exp\left(\frac{\mu_g - \mu_s}{kT}\right) - \exp\left(\frac{\mu_s - \mu_g}{kT}\right) \right] \quad (6)$$

where  $\mu_g$  and  $\mu_s$  are the chemical potentials of the gas and

adsorbed phases, respectively. The function  $K'_{gs}$  is the so-called equilibrium exchange rate. Equation 6 is valid for nondissociative adsorption only, whereas for dissociative adsorption, a similar balance between the chemical potentials must be preserved as in the equilibrium state. We have recently shown<sup>20,24</sup> that the form of eq 6 depends on the assumed rate-limiting step during dissociative adsorption. Previously,<sup>20</sup> we stated that this rate-limiting step for hydrogen adsorption on the Ni(100) surface is the disintegration of the activated complex and the forthcoming adsorption of hydrogen atoms. So, the difference between the chemical potentials under the exponents is of the form  $(\frac{1}{2}\mu_g - \mu_a)$ . In the opposite case (i.e., when the rate-limiting step is the creation of the activated complex), the difference would be following  $(\mu_g - 2\mu_a)$ .<sup>20,24</sup>

The equilibrium exchange rate describes the flux between phases at the hypothetical equilibrium state in an isolated system created by closing of the real open system at a given pressure and surface coverage, and allowing it to reach the equilibrium state.<sup>20–22,24,25</sup> The  $K'_{gs}$  is a function of temporal coverage and pressure and may be defined as follows:<sup>25</sup>

$$K'_{gs} = K_{gs} p^{(e)} S(\theta^{(e)}) \xi \quad (7)$$

where  $S$  is the conventional sticking coefficient,  $\theta^{(e)}$  is the equilibrium coverage in the isolated system,  $\xi$  is the probability of adsorption of a molecule when it strikes a free adsorption site, and  $p^{(e)}$  is the equilibrium pressure in the isolated system.  $K_{gs}$  is a constant parameter which is proportional to the collision frequency of the adsorbate molecules with the surface. Because all the components of  $K'_{gs}$  must be considered at equilibrium and for the isolated system, this function will also depend on the proportion between gaseous and adsorbed phases. More detailed information concerning the function  $K'_{gs}$  can be found elsewhere.<sup>20,22,24–26</sup>

In our previous publications concerning the kinetics of dissociative adsorption,<sup>20,24</sup> we found some analytical expressions describing the coverage and pressure dependence of the function  $K'_{gs}$ . These expressions were developed on the basis of mass balance between the gas and adsorbed phases and assuming equilibrium between molecular and atomic adsorption. Now, all the components of  $K'_{gs}$  are directly accessible from the simulations, so it is not necessary to derive any approximate expressions describing its functional form.

Taking advantage of the previous results<sup>20</sup> indicating that the adsorption system can be considered as *volume dominated* (i.e., the adsorption of hydrogen does not change the pressure of the gas phase over the surface), we can assume that  $p^{(e)} = p$ . Then, the equilibrium coverage in the hypothetical isolated system  $\theta^{(e)}$  is independent of the value of  $\theta$  in the open system and may be calculated from the adsorption isotherm

$$\mu_s(\theta^{(e)}) = kT \ln Kp \quad (8)$$

The coverage dependence of the sticking coefficient  $S(\theta)$  was derived from the simulations as the probability of finding an ensemble of sites where the dissociation and adsorption is possible. These are the sets of sites depicted in Figure 2. Let us recall that dissociation is possible only over the top site, and subsequent adsorption of two H atoms is possible on two HL (neighboring BR sites must be free) or BR (neighboring HL sites must be free) sites. In fact, we need a product  $S\xi$  as a function of pressure, because the experimental kinetic curves were determined at five different pressures of adsorbate and at constant temperature. The product  $S\xi$  was calculated as the ratio

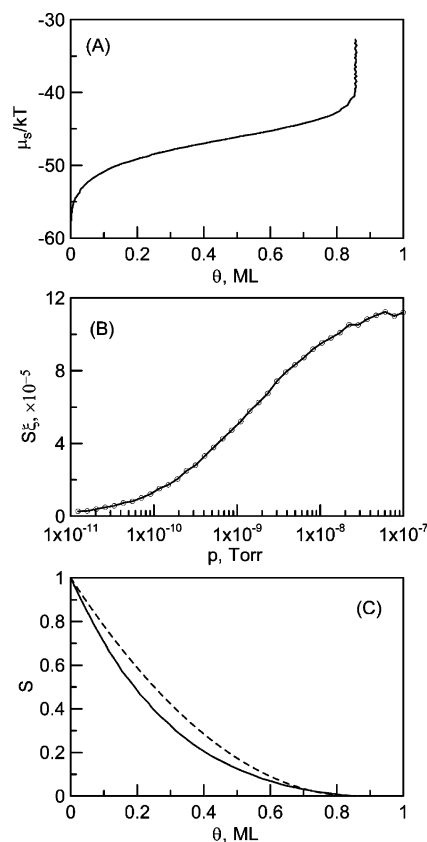


**Figure 8.** (A) The behavior of the chemical potential of the adsorbed phase at 300 K. The chemical potential of hydrogen atoms  $\mu_a = \frac{1}{2}\mu_s$ . (B) The product  $S\xi$  as a function of pressure at 300 K. Pressure is calculated on the basis of eq 4 where the value of  $K$  at 300 K is obtained from linear extrapolation shown in Figure 6B. (C) The behavior of the conventional sticking coefficient in the system  $H_2/Ni(100)$  (solid line); the dashed line shows the behavior of the standard expression for the dissociative adsorption, i.e.,  $(1 - \theta/\theta_s)^2$ .

of the successful dissociation/adsorption attempts to the total number of trials at a given value of  $\mu_s$ .

The SRT kinetic equation describing the time evolution of the coverage should, thus, be following

$$\frac{d\theta}{dt} = K_{gs} p S \xi \left[ \sqrt{Kp} e^{-\mu_s/2kT} - \frac{1}{\sqrt{Kp}} e^{\mu_s/2kT} \right] \quad (9)$$

and it should correctly predict the kinetics of adsorption, provided that the applied model of adsorption is correct. This equation contains one unknown parameter (i.e., the  $K_{gs}$ ), which is only temperature dependent. This parameter accounts for some factors which cannot be directly calculated and should be treated as an adjustable parameter. The most important components of  $K_{gs}$  are the probability of a correct orientation of the  $H_2$  molecule toward the surface, the initial sticking probability, the frequency of collisions of  $H_2$  molecules with the surface, and probably some other factors which cannot be easily accounted for.

Figure 8A shows the coverage dependence of  $\mu_s = 2\mu_a$  determined from simulations at  $T = 300$  K, whereas Figure 8B shows the behavior of the  $S\xi$  function also determined at 300 K (i.e., the temperature at which the experimental uptake curves were measured). In Figure 8C, the behavior of the conventional sticking coefficient is presented, indicating that  $S$  is not of the form  $(1 - \theta)^2$ , as is usually the case in dissociative adsorption. The sticking coefficient shown in Figure 8C was



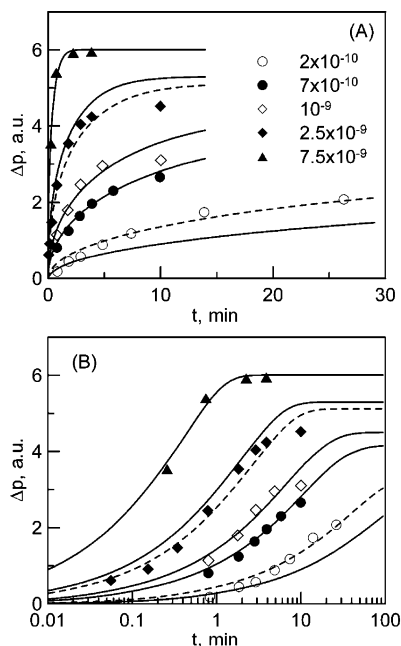


**Figure 9.** The comparison between the theoretical kinetics curves obtained using eq 9 (solid lines) and the experimental kinetic curves (symbols) reported by Christmann et al.<sup>4</sup> for five pressures shown in the legend in Torr units. The results plotted in linear (A) and logarithmic (B) scales. The adsorbed amounts were determined by the pressure increases  $\Delta p$  due to laser-induced thermal desorption. The dashed lines show the theoretical kinetic curves for slightly modified values of two pressures, i.e., for  $p = 3 \times 10^{-10}$  and  $2 \times 10^{-9}$  Torr. These values of pressure give theoretical kinetics which are a better match to the experimental kinetic curves for  $p = 2 \times 10^{-10}$  and  $2.5 \times 10^{-9}$  Torr. The theoretical kinetic isotherms were calculated assuming  $T = 300$  K,  $K = 1.57 \times 10^{-11}$  Torr $^{-1}$ ,  $K_{gs} = 2.5 \times 10^{11}$  ML/(min Torr), and 1 ML = 8 au.

determined as a fraction of the sites available for dissociation/adsorption, so its value at zero coverage does not correspond to the real initial sticking coefficient,  $S_0$ . Thus, the so-determined value of  $S$  may be called the normalized sticking coefficient.

The value of the parameter  $K$  which appears in kinetic eq 9 can be calculated for temperature 300 K using the linear approximation shown in Figure 6B. Its value at 300 K is  $1.57 \times 10^{-11}$  Torr $^{-1}$ . Equation 9 was next solved numerically to obtain the time evolution of the surface coverage and to compare the theoretical predictions with experiment. The results are shown in Figure 9 in linear (A) and logarithmic (B) scales. To compare the experimental kinetic curves with predictions given by eq 9, we need to express the arbitrary units used by Christman et al. in monolayers. To do this, we calculated the theoretical coverage for the highest experimental pressure ( $7.5 \times 10^{-9}$  Torr) from the isotherm shown in Figure 8A,  $\ln Kp = \ln[(1.57 \times 10^{-11}) \text{ Torr}^{-1} \times (7.5 \times 10^{-9}) \text{ Torr}] = -43.59 \Rightarrow \theta = 0.75$  ML. Looking at the kinetic isotherm for  $p = 7.5 \times 10^{-9}$  Torr, we can see the plateau indicating that at time of ca. 5 min the equilibrium is just established. So, we can assume that 6 au corresponds to 0.75 ML (i.e., 1 ML = 8 au).

Next, we adjusted the parameter  $K_{gs}$  in order to obtain the best match between theoretical and experimental kinetic isotherms. Because the parameter  $K_{gs}$  is only temperature dependent, its value should be the same for all investigated pressures. This best value of  $K_{gs}$  was estimated to be  $2.5 \times 10^{11}$  ML/(min Torr).

The solid lines in Figures 9 show the prediction given by eq 9; as can be seen, this prediction is very good, because the only

one parameter for all curves was adjusted. The agreement between theory and experiment is worse for  $p = 2 \times 10^{-10}$  Torr and  $p = 2.5 \times 10^{-9}$  Torr. A slight modification of these values results in much better agreement between theoretical and experimental kinetic curves, as shown by the dashed lines. These modified values of pressure are  $3 \times 10^{-10}$  and  $2.0 \times 10^{-9}$  Torr.

Thus, we can also state that the adsorption kinetics of hydrogen on Ni(100) confirms the validity of our model, because most of the components of the SRT kinetic equation were taken from the simulations. The results shown in Figure 9 also support the application of the SRT approach in theoretical studies of the kinetics of adsorption.

## Summary and Conclusions

In this work, we proposed the thermodynamic model of adsorption of hydrogen on the (100) nickel single-crystal face. Taking advantage of the DFT results, we assumed that dissociation of the hydrogen molecule is possible only when the molecule approaches the surface with its center of mass over the topmost nickel atom. The second important assumption is that the hydrogen atoms may adsorb either on the hollow sites (assumed binding energy  $\epsilon_H = -48$  kJ/mol H) or on the bridge site ( $\epsilon_B = -37$  kJ/mol H). We have arrived at a reasonable mechanistic model of hydrogen adsorption on Ni(100) that is able to capture most of the experimentally observed results. The proposed model consists of the following assumptions:

1. The dissociation of the incoming hydrogen molecule is possible only when the H atoms are oriented toward two free HL (BR) sites and all the adjacent BR (HL) sites are not occupied by the already adsorbed H atoms.
2. The adsorbed hydrogen atoms may migrate on the surface (jumps from the HL sites into the BR sites, or from the BR sites into the HL sites) with probability depending on the local binding energy and on the relative rate of diffusion,  $P_{\text{diff}}$ , so the hydrogen atoms are neither completely free nor localized on the surface.
3. There is no lateral interaction between adsorbed hydrogen atoms.
4. The adsorption on the BR sites is the intermediate state for diffusion and desorption.
5. The associative desorption of hydrogen is possible only when two H atoms meet on the adjacent HL and BR sites.

The above features of the model imply that the presence of the adsorbed H atom modifies the electronic structure of the adjacent topmost atoms in such a way that the dissociation of the hydrogen molecule over these atoms is no longer possible. Therefore, at higher coverages (high values of  $\mu_a$ ), the number of the ensembles of sites suitable for dissociation becomes very small. On the other hand, the probability of adsorption increases (see eq 1). As a result, a steady-state value of the coverage is established, that is, the saturation coverage  $\theta_s = 0.858$  ML.

Because the rate of associative desorption is limited by the rate of diffusion, the predicted isotherms of adsorption become steeper as the temperature decreases. This explains the intriguing behavior of the experimental adsorption isotherms, plotted in the form  $\ln \theta/(\theta_s - \theta)$  versus  $\ln p$ , indicating a similar decrease of the slopes with increasing adsorption temperature. At very low temperatures, the rate of diffusion becomes very small, and consequently, the desorption of hydrogen is practically disabled. So, at low temperatures, the adsorption of hydrogen is essentially irreversible.

The determined probability of diffusion  $P_{\text{diff}} = 0.04$  implies that hydrogen atoms are not fully mobile on the surface; however, they cannot be treated as localized, at least at room and elevated temperatures.



Thus, our model explains why the saturation coverage of hydrogen on Ni(100) is lower than unity and the adsorbed layer is not ordered at saturation or at elevated temperatures. It also explains the decreasing tendency of the slopes of the adsorption isotherms with increasing temperature. In turn, this model cannot explain the behavior of the heat of adsorption for high coverages (close to saturation). However, we suspect that the decrease of the heat of adsorption at high coverages is mainly due to the lack of proportionality between  $\Delta\varphi$  and  $\theta$ . Also, it is not clear if the work function itself is independent of temperature at higher coverages. Both these factors make the experimental heat of adsorption (determined from the Clausius–Clapeyron equation) uncertain for high coverages.

The analysis of the adsorption kinetics, based on the application of the SRT approach, gives additional support for the validity of our model of hydrogen adsorption on Ni(100). Moreover, the form of the SRT equation suggests that the rate-limiting step during the dissociation and adsorption of hydrogen is the disintegration of the activated complex and the forthcoming adsorption of the H atoms. The other form of the SRT equation (i.e., corresponding to the situation when the rate-limiting step is the creation of the activated complex) is not able to recover the experimental uptake curves.

**Acknowledgment.** This work was supported by the Polish State Committee for Scientific Research grant 4 T09A 015 24. One of the authors (P.S.) is grateful to the Foundation for Polish Science (FNP) for the Award of a Stipend for Young Scientists. The authors thank Prof. A. Patrykiewicz for helpful discussions.

## References and Notes

- (1) Kresse, G.; Hafner, J. *Surf. Sci.* **2000**, 459, 287.
- (2) Lapujoulade, J.; Neil, K. S. *J. Chem. Phys.* **1972**, 57, 3535.
- (3) Lapujoulade, J.; Neil, K. S. *Surf. Sci.* **1973**, 35, 288.
- (4) Christmann, K.; Schober, O.; Ertl, G.; Neumann, M. *J. Chem. Phys.* **1974**, 60, 4528.
- (5) Winkler, A.; Rendulic, K. D. *Surf. Sci.* **1982**, 118, 19.
- (6) Christmann, K.; Ertl, G.; Schober, O. *Surf. Sci.* **1973**, 40, 61.
- (7) Rieder, K. H.; Wilsch, H. *Surf. Sci.* **1983**, 131, 245.
- (8) Guvenc, Z. B.; Guvenc, D. *Surf. Sci.* **2003**, 529, 11.
- (9) Kammler, T.; Wehner, S.; Kuppers, J. *Surf. Sci.* **1995**, 339, 125.
- (10) Christmann, K. *Z. Naturforsch.* **1979**, 34a, 22.
- (11) Kammler, T.; Lee, J.; Kuppers, J. *J. Chem. Phys.* **1997**, 106, 7362.
- (12) Eilmsteiner, G.; Walkner, W.; Winkler, A. *Surf. Sci.* **1996**, 352–354, 263.
- (13) Winkler, A. *Appl. Phys. A* **1998**, 67, 637.
- (14) Premm, H.; Polzl, H.; Winkler, A. *Surf. Sci.* **1998**, 401, L444.
- (15) Johnson, S.; Madix, R. J. *Surf. Sci.* **1981**, 108, 77.
- (16) Cerofolini, G. F.; Rudzinski, W. Theoretical Principles of Single- and Mixed-Gas Adsorption Equilibria on Heterogeneous Solid Surfaces. In *Equilibria and Dynamics of Gas Adsorption on Heterogeneous Solid Surfaces*; Rudzinski, W., Steele, W. A., Zgrablich, G., Eds.; Elsevier: Amsterdam, 1997.
- (17) Halsey, G. D. *J. Chem. Phys.* **1976**, 65, 2029.
- (18) Kresse, G. *Phys. Rev. B* **2000**, 62, 8295.
- (19) Rendulic, K. D.; Anger, G.; Winkler, A. *Surf. Sci.* **1989**, 208, 404.
- (20) Panczyk, T.; Rudzinski, W. *Appl. Surf. Sci.* **2004**, 233, 141.
- (21) Ward, C. A.; Findlay, R. D.; Rizk, M. *J. Chem. Phys.* **1982**, 76, 5599.
- (22) Elliot, J. A. W.; Ward, C. A. *J. Chem. Phys.* **1997**, 106, 5667.
- (23) Rudzinski, W.; Everett, D. H. *Adsorption of Gases on Heterogeneous Surfaces*; Academic Press: London, 1992.
- (24) Panczyk, T.; Rudzinski, W. *J. Phys. Chem. B* **2004**, 108, 2898.
- (25) Elliott, J. A. W.; Ward, C. A. Statistical Rate Theory and the Material Properties Controlling Adsorption Kinetics. In *Equilibria and Dynamics of Gas Adsorption on Heterogeneous Solid Surfaces*; Rudzinski, W., Steele, W. A., Zgrablich, G., Eds.; Elsevier: Amsterdam, 1997.
- (26) Panczyk, T. *Appl. Surf. Sci.* **2004**, 222, 307.